Eng. Sci., 2022, **18**, 105–112

Engineered Science

DOI: https://dx.doi.org/10.30919/es8d626

New Pressure Matrix Array Sensor Composed of Flexible Mechanical Sensor Elements

Yufeng Wu,[1,#] Junchen Liu,[1,#] Sen Lin,[2] Kun Huang,[1] Enfu Chen,[1] Kai Huang[1] and Ming Lei[1,*]

Abstract

Due to the development of science and technology, people are increasingly interested in portable and flexible devices, and demand is deepening. Among them, sensors play an important role in signal transmission between people and equipment. We study a low-cost, easy-to-prepare, and can-be mass-produced flexible pressure sensor element, which is made of silver nanowires/polyvinyl butyral/melamine sponge (AgPMS). Due to the chemical stability of the silver nanowires and its wrapped structure on the melamine sponge skeleton, AgPMS can maintain constant resistance in 5000 times compression and at high temperatures for 15 days, indicating high mechanical stability and high oxidation resistance. With the 60% compression, AgPMS shows a 60% high resistance change rate. To apply it to actual sensing, we assembled the AgPMS into a 5 × 5 sensor matrix array (SMA). It shows the sharp difference in resistance change rate while under compression of 30% and 60%. We compare the force distribution exhibited by several different shapes of pressure, respectively. It indicates that each array element has high responsiveness to the resistance changes. And the sensitivity can be adjusted freely with the array size of the sensor.

Keywords: Sensor matric array; Flexible; Silver nanowires; Stability; Pressure.
Received: 09 June 2021; Revised: 18 July 2021; Accepted: 05 August 2021.
Article type: Research article.

1. Introduction

Nowadays, due to the development and combination of electronic technology and biology, there has been growing interest in flexible and portable devices such as electronic skins (e-skins),[1-10] health-monitoring devices[11-14] and artificial muscles,[15-17] And it may be used in the field of brain-computer interfaces[18-20] in the future. For example, high-sensitive pressure sensors could be used in the continuous recording of pulse and blood pressure for the collection of fundamental health information.[21] Thus, people are gradually realizing the importance of pressure sensors and it becomes the focus of research. Through nearly a decade of scientific research, various pressure sensors have been developed based on the sensing mechanisms of piezoresistivity,[22,23] capacitance,[24-26] piezoelectricity,[27] and field-effect transistor (FET).[7,8,10] People use them to collect electrical signals which are converted from mechanical signals. Importantly, each of them has a different scope of application.

Nevertheless, while these types of sensors show obvious advantages, they will also reveal some drawbacks. Piezoresistive type sensor has a simple structure and readout, fast response speeds, and low-temperature sensitivity.[1] But it shows drift and hysteresis. The capacitive-type sensor has high strain sensitivity, compatibility with static force measurement, and low power consumption. The most critical problem is that it is susceptible to interference from external circumstances. The piezoelectric-type sensor has a high sensitivity to dynamic pressure and fast response speed.[10] On the contrary, it is unreliable in static sensing. It is worth mentioning that FET-type pressure sensors can take advantage of active-matrix sensors, which can provide high-quality sensing and reduce crosstalk between pixels.[28] The FET-type pressure sensor is expected to enable advanced sensing performance, including multi-parameter monitoring, high sensitivity and resolution, and a low degree of signal crosstalk relative to the capacitive-type sensor.[7] However, the high cost and technical difficulties are problems that have not yet been solved.

There are some research hotpots in the sensor field. First,

[1] *State Key Laboratory of Information Photonics and Optical Communications, School of Science, Beijing University of Posts and Telecommunications, Beijing 100876, China.*

[2] *School of Physical Science and Technology, Guangxi University, Nanning 530004, China.*

[#] *These authors contributed to this work equally.*

* *E-mail:* mlei@bupt.edu.cn (M. Lei)

sensors are expected to be versatile and can enable the perception of pressure, bending, torsional forces, and acoustic vibrations.[2] Second, it is to make the sensors both flexible and strong and can adapt to a variety of use or environment, like different temperatures and air pressure conditions.[21,29] Third, sensors should be reusable, retain their functionality and reliability under large mechanical deformation,[4] and have high stability, like oxidation resistance. Forth, it is important to reduce the production cost and difficulty of manufacturing sensors on an industrial scale.[21]

Herein, we report a facile, inexpensive, and scalable method for flexible mechanical sensor elements AgPMS, which can be further formed into an array sensor through a certain assembly. The new electrode material consists of a commercial melamine sponge (MS), which is fully infiltrated with prefabricated silver nanowires (AgNWs) and polyvinyl butyral (PVB) solution[30-32] during a vacuum processing step. After 5 min in a 1 000 Pa vacuum, a metalized melamine sponge is obtained (Fig. 1). Lots of metalized melamine sponges can be produced simultaneously by batch pre-punching the melamine sponge into precursors of a specified size, allowing for mass production. Benefiting from the micron-sized sponge structure of the melamine sponge, the AgPMS is ultralight (20.4 mg/cm^3), which makes them easy to transport or carry. It has a high rate of resistance change (~60%), high electric stability (1000 cycles of cyclic voltammetry (CV)), can stable resistance for 5 000 times 60% compression tests, and a high temperature (80 ℃) for at least 15 days. This method reduces the cost and difficulty of fabrication while maintaining significant electrical, chemical and mechanical stability. The strain sensitivity can be optimized by controlling the doping quality of silver nanowires. We show the fabrication of AgPMS by sponge metallization under mild conditions and the assembly of pressure sensors. Importantly, we demonstrate the sensing performance of SMA by applying different pressure to different pixel points.[33,34] The sensor can make a relatively obvious response to the strength of the current signal caused by the change in pressure. The advantage of it is that its accuracy can be adjusted freely according to the application requirements. As the array size increases, the precision of SMA will also improve. The substrate of SMA is made of polylactic acid (PLA) and can be also kept at 80 ℃ without softening.

2. Experimental section

2.1 Materials

Polyvinyl butyral (PVB, Mw=170 000), polyvinylpyrrolidone (PVP, Mw=360 000), ethanol (GR, moisture content<0.2%), silver nitrate ($AgNO_3$, 99.8%), cupric chloride dihydrate ($CuCl_2·2H_2O$, AR) and sodium chloride (NaCl, 99.5%) were purchased from Aladdin. Acetone (99.5%) is purchased from Modern Oriental (Beijing) Technology Development Co. Ltd. Melamine sponges and 3-dimension-printable PLA are commercially available.

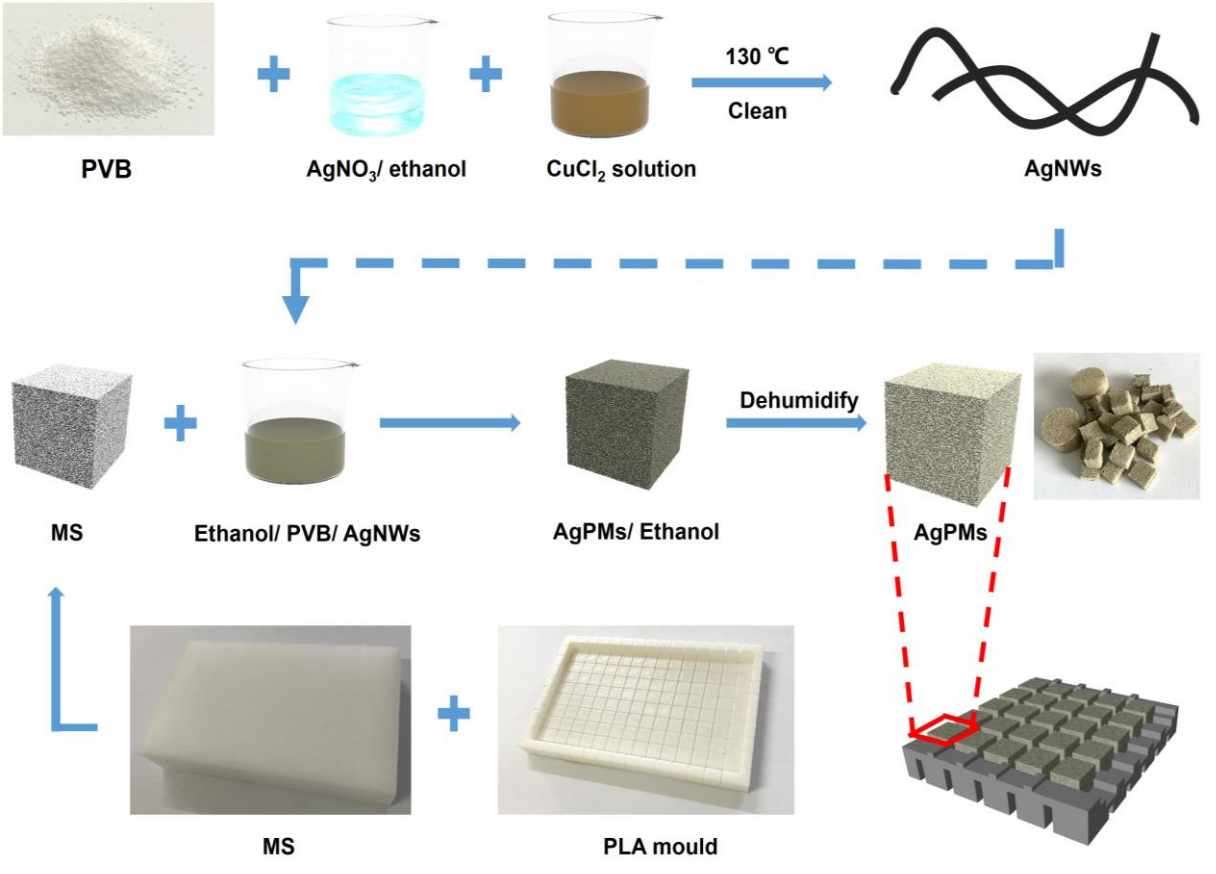

Fig. 1 Preparation and application of flexible mechanical sensor element, and structure of SMA.

2.2 Synthesis of AgNWs

0.4 g of polyvinylpyrrolidone (PVP, Mw = 360000) and 0.5 g of silver nitrate ($AgNO_3$) were sequentially dissolved in 100 mL of ethanol under magnetic stirring. After being thoroughly dissolved, 0.8 mL of an as-prepared $CuCl_2 \cdot 2H_2O$ (3.3 mM) / ethanol solution was rapidly injected into the mixture and gently stirred. Next, the mixture was immersed in a preheated silicone oil bath at 130 °C for 3 h. Finally, the resulting solution was cleaned three times with acetone and ethanol with centrifugation at 3000 rpm for 10 min. The resultant AgNWs were dispersed in ethanol, forming a 100 mg/g AgNWs/ethanol solution for further use.[18] It is generally diluted into silver nanowires/alcohol solution of 20 mg/ml when we use it.

2.3 Preparation of AgPMS

In a pre-treatment process, some sponge was first cut into 0.7 cm × 0.7 cm × 0.5 cm blocks by the 3D printed mold. Second, 0.5 g of PVB was dissolved in 99.5 g ethanol to prepare 0.5 wt.% PVB/ethanol solution and stirred at 25 °C for 6 hours. Then 1.0 g AgNWs/ethanol solution (20 mg/ml) was added into 9.0 g PVB/ethanol solution and stirred for 10 min. At last, dip the treated sponges into the AgNWs/PVB/ ethanol solution and underwent a vacuum treatment at 1 000 Pa for 5 min.[35,36] The AgPMS were finally obtained after natural drying. They are used for assembling sensors.

And another part of the sponge will be made into a cylinder with a diameter of 1.7 cm and a height of 1 cm in the pre-treatment process. The next steps are the same as above. They are used for electrical, mechanical, and chemical stability tests.

2.4 Design and assembly of SMA

The sensor matrix array is 3D printed using polylactic acid (PLA) material. The element slot is designed to be 0.7 cm × 0.7 cm × 0.2 cm. The connection position of the signal clamp has been designed in advance on the SMA.

First, the copper tape is attached to the channel of the array. Then put the sensor element into the element slot, and another layer of copper tape is attached. The upper and lower layers of tape are perpendicular to each other so that the position of pressure can be determined using coordinates.

2.5 Micromorphological characterization

X-ray powder diffraction data were collected using diffraction of X-rays (XRD, D/max 2 500, Rigaku, Japan) with Cu Kα radiation (λ = 1.54178 Å). Micromorphological images were recorded using a field emission scanning electron microscope (FE-SEM, LEO-1 530, Zeiss, Germany) with an EDX attachment module. An X-ray photoelectron spectrometer (Escalab 250Xi, Thermo Fisher, America) equipped with an Al Kα radiation source (1 487.6 eV) and a hemispherical analyzer with a pass energy of 30.00 eV was employed to obtain surface element information. The thermogravimetric analysis (TGA) and differential thermal gravity (DTG) analysis were performed using a thermogravimetric analyzer (STA 449 F3, Jupiter, Germany).

2.6 Mechanical properties

The mechanical stability of the AgPMS was measured at room temperature using a static testing system in cyclic compression mode (ZwickRoell 1 kN, Germany) combined with a computer-controlled electrochemical workstation (CHI 660E, CH Instrument, China).

2.7 Electrical properties

The measurement of the electrical conductivity of the AgPMS, CV, and linear sweep voltammetry (LSV) was taken from a computer-controlled electrochemical workstation (CHI 660E, CH Instrument, China). Arduino and chips (CD4067BE) are used in electrical signal testing to provide a path and brake control for the circuit. As the conductivity of AgPMS is isotropous, we use a cylindrical AgPMS for testing, it can be calculated by the following equation:

$$R = \rho \frac{L}{S} = \frac{U}{I} \quad (1)$$

$$\sigma = \frac{1}{\rho} \quad (2)$$

$$\sigma = \frac{LI}{US} \quad (3)$$

where σ is the conductivity, L is the length of the AgPMS, S is the cross-sectional area of the AgPMS, and U and I are the applied voltage and the corresponding current which is available through the electrochemical workstation, respectively. In the sensing performance tests of SMA, we also manually measure the change of resistance through the electrochemical workstation to ensure the accuracy of the test data.

3. Results and discussion

AgPMS is consist of self-locking silver nanowires, a micron-sized melamine sponge skeleton, and PVB (Figs. 2a, 2b). The function of self-locking silver nanowires is for electrical conduction. The sponge skeleton is for mechanical support because of its flexibility and elasticity. And PVB is for the adhesion between the AgNWs and the sponge skeleton. However, a thick and insulating PVB layer could appear due to film formation near any residual air in the melamine sponge[18]. Therefore, an additional vacuum treatment is necessary to completely remove the air. The TGA and DTG analyses indicate that AgPMS prepared by the synthesis method in this paper is loaded with about 7 wt.% Ag. The high load of Ag makes the electrical signal have a small loss in the transmission process. X-ray photoelectron spectroscopy (XPS) analysis of the AgPMS shows that both Ag and PVB were loaded on the sponge (Figs. 2c, 2d), suggesting that a highly conductive surface with a trace of the polymer coating is present in the insulated melamine sponge. The peaks at 368.8 eV and 374.8 eV both correspond to Ag, and the peaks at 367.7 eV and 373.7 eV correspond to lose features, which are observed to higher binding energy side of each spin-orbit component for Ag metal. And the peaks at 286.1 eV and 288.6 eV correspond to C-O-C and O-C=O bonds in PVB,

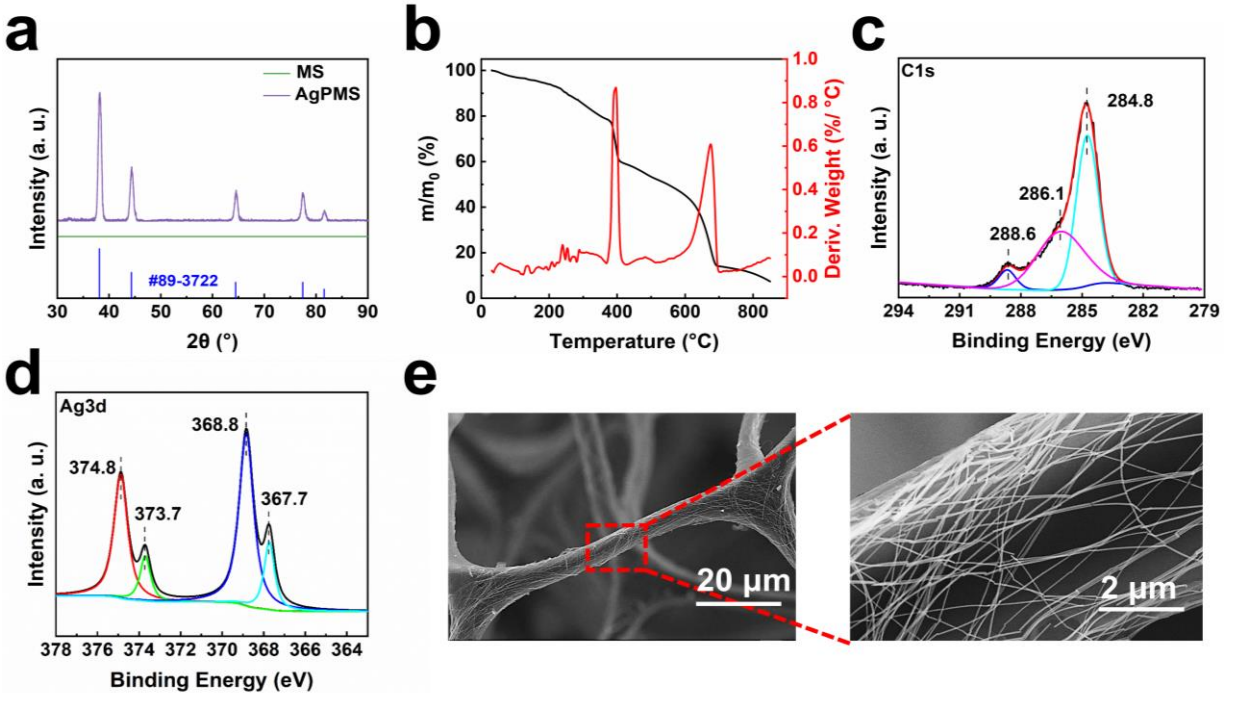

Fig. 2 (a) XRD pattern of the AgPMS and melamine sponge; (b) TG (black) and DTG (red) of the AgPMS; XPS peak-differentiation-imitating analysis of (c) C1s and (d) Ag3d performed on the AgPMS; (e) SEM images of the AgPMS.

respectively. Meanwhile, AgNWs are wound on the MS skeleton (Fig. 2e). The reason for this structure is that AgNWs are long and wound under the combined action of vacuum treatment and PVB. This winding structure prevents the AgNWs from falling off easily when AgPMS is under pressure and helps to stabilize the signal transmission under repetitive compression.

Electric performance is a key factor of sensors for signal recording. AgPMS has different conductivity (σ) because of the precursor solutions with different silver content (Fig. 3a), which is 1 wt.%, 2.5 wt.%, 5 wt.%, 10 wt.% and 20 wt.%, respectively. The results showed the higher the silver content, the higher σ was, indicating that the conductivity was adjustable and depends on the mass ratio of the AgNWs. The AgPMS shows a linear conduction characteristic with a stable resistance for a 1 000-cycle voltammetry (CV) test (Fig. 3b). The LSV characteristics (Fig. 3c) of the AgPMS suggest that the resistance could be stable at the same compression, and the resistance responded differently when compression changed. The change in the resistance value comes from the change in the silver density in AgPMS. The silver density increased during compression, which leads to an increase in the electrical conductivity and resistance change rate.[18,37] The oxidization of metal-based electrode materials is a critical problem for long-term operations. Thus, to investigate the oxidization ability, we then performed accelerated oxidation experiments on AgPMS at 80 °C for 15 days (Fig. 3d). The result showed that the resistance did not change in such an environment. Flexibility and mechanical stability are two other important properties of AgPMS. We test the direct relationship between the force and the compression (Fig. 3e). The microstructure of a sponge is not destroyed during compression. We performed repeated compression experiments on the AgPMS to test its long-term mechanical stability, and flexibility (Figs. 3f-3h). The resistance of the AgPMS remains unchanged after 5 000 cycles with a 15% compression ratio. Under more extreme conditions, the resistance of the AgPMS increases only by 8% with a 60% compression ratio. The high mechanical stability of the AgPMS is mainly due to the initial bendability of the one-dimensional silver and the mechanical support provided by the melamine sponge skeleton.[38] It is worth mentioning that the highest resistance change rate was approximately 60%, which was tested with a 60% compression. Even after 5 000 cycles, it can still have a 60% resistance change rate. Such a high resistance change rate provides support for a wide range of AgPMS applications.

We assembled the AgPMS into a pressure-resistance 5×5 sensor matrix array (SMA) (Figs. 4a, 4b). The structure of SMA consists of four parts: a PLA substrate, AgPMS, and two layers of perpendicular copper tape for signal transmission. We use matrix form to number the AgPMS in different positions (Fig. 4c). To prove the AgPMS has the same flexibility as a single element after assembling into an SMA, we did a mechanical test which suggested flexibility of AgPMS is completely retained in SMA.

Then, we design a circuit connection for testing the signal transmission of the SMA (Fig. 4e). We connect the signal output port of the microprogrammed control unit (MCU), Arduino, with the signal input ports of the two analog switches, firstly. High-level and low-level output signals, which are in the form of 1 and 0, respectively, are transmitted to the

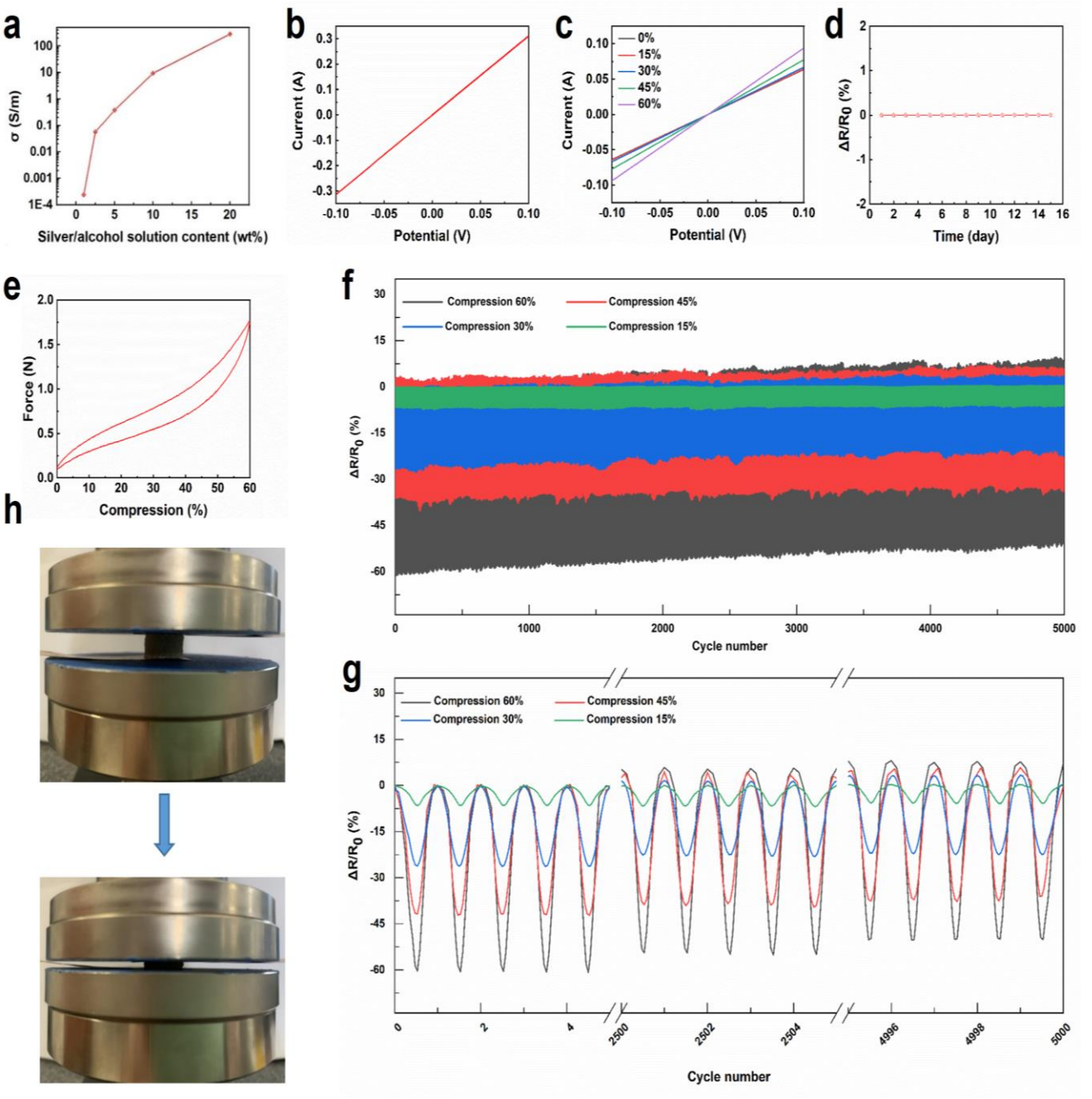

Fig. 3 (a) The conductivity varies with silver content, (b) 1000 cycles of CV, (c) The LSV for different compression ratios (15%, 30%, 45%, and 60%), and (d) The accelerated oxidation experiment performed in air at 80 °C of AgPMS; (e) The relation between element compression and shape variable; (f) The resistance change rate of 5000 cycles with different compression ratios were recorded by electrochemical workstation; (g) Details of the resistance rate change curve; (h) Photographs of the mechanical stability test setup for AgPMS in its initial state and 60% compressed state.

switches by program control. The various permutations and combinations of the input signals correspond to the switches with different pins. We control the rows and columns of the SMA with two switches, respectively. It is similar to when the two pins connecting the first row and the first column are on at the same time, we can obtain the resistance of the (1, 1) coordinate. Next, we use a regulated power supply to provide the working voltage for two switches. We used a computer-controlled electrochemical workstation to obtain the resistance of each position sensor element. They exhibit different rates of resistance change for different pressures (Figs. 4f, 4g). Furthermore, we demonstrate the resistance of SAM under different shapes of pressure (Fig. 4h).[39] We made four models of the letters "b", "u", "p" and "t" by 3D printing and overlaid them on SAM, respectively. By comparing the resistance change rates of covered and uncovered elements, the results indicated that the SMA can discriminate the pressure of different shapes. With the increase in array size, SMA could be more accurate in pressure position resolution.

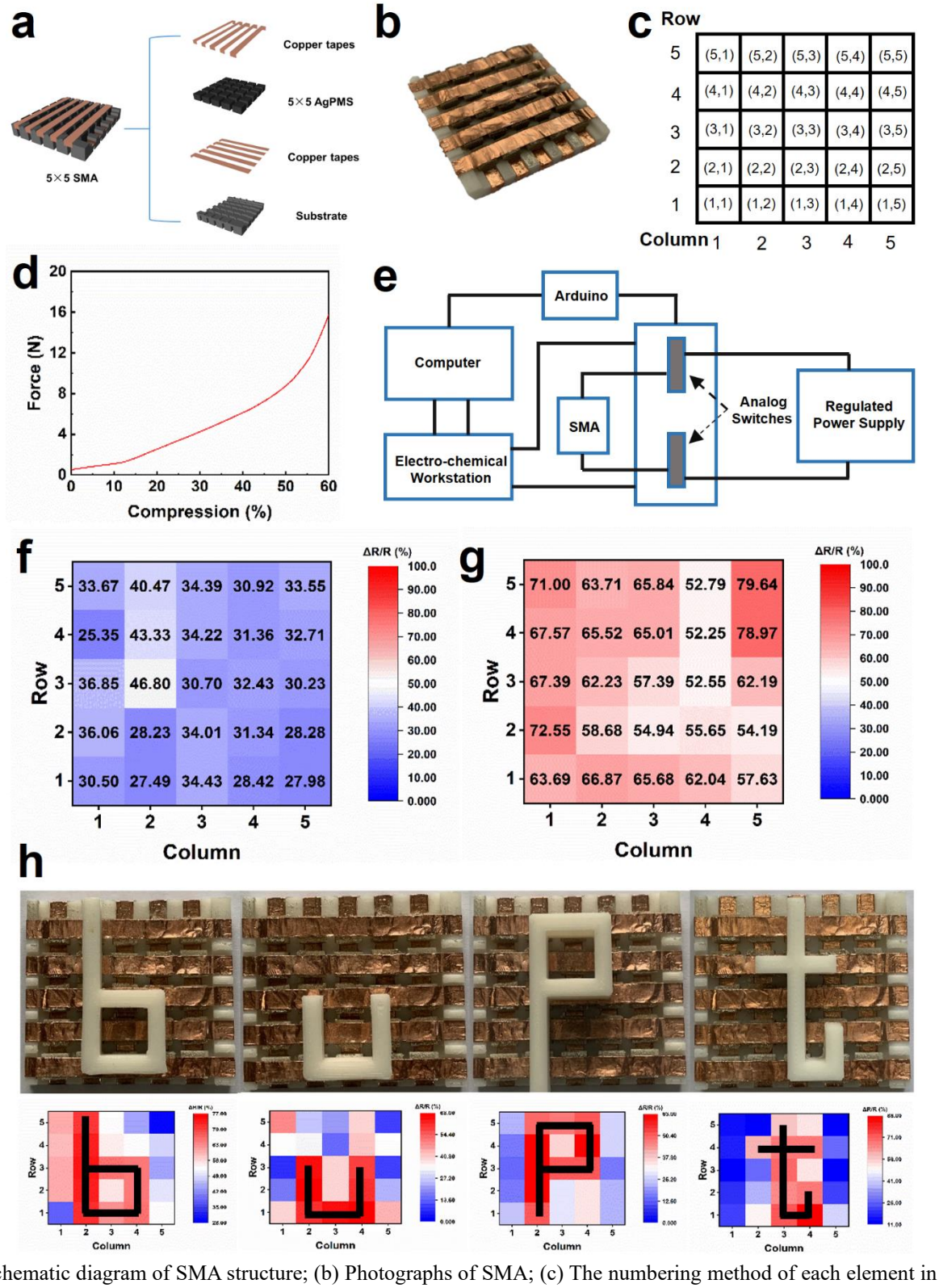

Fig. 4 (a) Schematic diagram of SMA structure; (b) Photographs of SMA; (c) The numbering method of each element in the SMA; (d) The relation between compression and shape variable; (e) Schematic diagram of SMA test circuit connection; Resistance change rate of each element under (f) 30% compression and (g) 60% compression; (h) Sensor performance demonstration.

4. Conclusions

In summary, we successfully prepared a flexible mechanical sensor element AgPMS with a facile, inexpensive, and scalable method. The experiments show the AgPMS has excellent electrical, chemical, and mechanical stability. Its resistance change rate is high enough to be used in a pressure sensor. In addition, we also successfully assemble the SMA, which can discriminate the pressure of different shapes. And we can freely control the resolution of the SMA by adjusting its size, with the increase in size, SMA could be more accurate.

We envision that AgPMS is a solution to the problem that sensor components cannot be manufactured on a large scale, and SMA could be used more in pressure sensing due to its stability under 5000 times 60% compression.

Acknowledgments
This study was supported financially by the Fundamental Research Funds for the Central Universities (2021XD-A04-1), the National Natural Science Foundation of China (Nos. 61874014 and 61874013), and the Fund of State Key Laboratory of Information Photonics and Optical Communications (Beijing University of Posts and Telecommunications, P.R. China).

Conflict of interest
There are no conflicts to declare.

Supporting information
Not Applicable.

References
[1] M. Hammock, A. Chortos, B. Tee, J. Tok, Z. Bao, *Advanced Materials*, 2013, **25**, 5997-6038, doi: 10.1002/adma.201302240.
[2] J. Park, Y. Lee, J. Hong, Y. Lee, M. Ha, Y. Jung, H. Lim, S. Kim, H. Ko, *ACS Nano*, 2014, **8**, 12020-12029, doi: 10.1021/nn505953t.
[3] W.-Y. Chang, T.-H. Fang, H.-J. Lin, Y.-T. Shen, Y.-C. Lin, *Journal of Display Technology*, 2009, **5**, 178-183, doi: 10.1109/jdt.2008.2004862.
[4] S. Wu, S. Peng, Y. Yu, C. Wang, *Advanced Materials Technologies*, 2020, **5**, 190090, doi: 10.1002/admt.201900908.
[5] H. Tian, Y. Shu, X. Wang, M. Mohammad, Z. Bie, Q. Xie, C. Li, W. Mi, Y. Yang, T. Ren, *Scientific Reports*, 2015, **5**, 8603, doi: 10.1038/srep08603.
[6] S. Jung, J. Kim, J. Kim, S. Choi, J. Lee, I. Park, T. Hyeon, D. Kim, *Advanced Materials*, 2014, **26**, 4825-4830, doi: 10.1002/adma.201401364.
[7] Q. Sun, D. H. Kim, S. S. Park, N. Y. Lee, Y. Zhang, J. H. Lee, K. Cho, J. H. Cho, *Advanced Materials*, 2014, **26**, 4735-4740, doi: 10.1002/adma.201400918.
[8] L. Lin, Y. Xie, S. Wang, W. Wu, S. Niu, X. Wen, Z. Wang, *ACS Nano*, 2013, **7**, 8266-8274, doi: 10.1021/nn4037514.
[9] W. Wu, X. Wen, Z. Wang, *Science*, 2013, **340**, 952-957, doi: 10.1126/science.1234855.
[10] S. Shin, S. Ji, S. Choi, K. Pyo1, B. An, J. Park, J. Kim, J. Kim, K. Lee, S. Kwon, J. Heo, B. Park, J. Park, *Nature Communications*, 2017, **8**, 14950, doi: 10.1038/ncomms14950.
[11] K. Takei, W. Honda, S. Harada, T. Arie, S. Akita, *Advanced Healthcare Materials*, 2015, **4**, 487-500, doi: 10.1002/adhm.201400546.
[12] H. Xu, Y. Lu, J. Xiang, M. Zhang, Y. Zhao, Z. Xie, Z. Gu, *Nanoscale*, 2018, **10**, 2090-2098, doi: 10.1039/c7nr07225b.
[13] C. Delebarre, S. Grondel, F. Rivart, *Advances in Applied Ceramics*, 2015, **114**, 205-210, doi: 10.1179/1743676114y.0000000220.
[14] S. Nag-Chowdhury, H. Bellegou, I. Pillin, M. Castro, P. Longrais, J. F. Feller, *Composites Science and Technology*, 2016, **123**, 286-294, doi: 10.1016/j.compscitech.2016.01.004.
[15] Y. Park, R. Wood, *IEEE Sensors Journal*, 2013, **3**, 6688298, doi: 10.1109/ICSENS.2013.6688298.
[16] B. Tondu, *Journal of Intelligent Material Systems and Structures*, 2012, **23**, 225-253, doi: 10.1177/1045389X11435435.
[17] H. Fujisue, T. Sendai, K. Yamato, W. Takashima, K. Kaneto, *Bioinspiration & Biomimetics*, 2007, **2**, S1-S5, doi: 10.1088/1748-3182/2/2/s01.
[18] S. Lin, J. Liu, W. Li, D. Wang, Y. Huang, C. Jia, Z. Li, M. Murtaza, H. Wang, J. Song, Z. Liu, K. Huang, Di Zu, M. Lei, B. Hong, H. Wu, *Nano Letters*, 2019, **19**, 6853-6861, doi: 10.1021/acs.nanolett.9b02019.
[19] M. Treder, N. Schmidt, B. Blankertz, *Journal of Neural Engineering*, 2011, **8**, 066003, doi: 10.1088/1741-2560/8/6/066003.
[20] N. Birbaumer, *Psychophysiology*, 2006, **43**, 517-532, doi: 10.1111/j.1469-8986.2006.00456.x.
[21] Y. Zang, F. Zhang, C.-A. Di, D. Zhu, *Materials Horizons*, 2015, **2**, 140-156, doi: 10.1039/c4mh00147h.
[22] W. Mahmoud, A. El-Lawindy, M. El Eraki, H. Hassan, *Sensors and Actuators A: Physical*, 2007, **136**, 229-233, doi: 10.1016/j.sna.2006.11.017.
[23] L. Pan, A. Chortos, G. Yu, Y. Wang, S. Isaacson, R. Allen, Y. Shi, R. Dauskardt, Z. Bao, *Nature Communications*, 2014, **5**, 3002, doi: 10.1038/ncomms4002.
[24] K. Li, H. Wei, W. Liu, H. Meng, P. Zhang, C. Yan, *Nanotechnology*, 2018, **29**, 185501, doi: 10.1088/1361-6528/aaafa5.
[25] J. Feng, X. Kang, Q. Zuo, C. Yuan, W. Wang, Y. Zhao, L. Zhu, H. Lu, J. Chen, *Sensors*, 2016, **16**, 314, doi: 10.3390/s16030314.
[26] M. Kang, J. Kim, B. Jang, Y. Chae, J. Kim, J. Ahn, *ACS Nano*, 2017, **11**, 7950-7957, doi: 10.1021/acsnano.7b02474.
[27] B. You, C. Han, Y. Kim, B. Ju, J. Kim, *Journal of Materials Chemistry A*, 2016, **4**, 10435-10443, doi: 10.1039/c6ta02449a.
[28] J. Oh, D. Son, T. Katsumata, Y. Lee, Y. Kim, J. Lopez, H. Wu, J. Kang, J. Park, X. Gu, J. Mun, N. Wang, Y. Yin, W. Cai, Y. Yun, J. Tok, Z. Bao, *Science Advances*, 2019, **5**, eaav3097, doi: 10.1126/sciadv.aav3097.
[29] K. Bi, Q. Wang, J. Xu, L. Chen, C. Lan, M. Lei, *Advanced Optical Materials*, 2021, **9**, 2001474, doi: 10.1002/adom.202001474.
[30] B. Song, W.-Y. Lu, C. J. Syn, W. Chen, *Journal of Materials Science*, 2009, **44**, 351-357, doi: 10.1007/s10853-008-3105-0.
[31] S. Lin, H. Wang, F. Wu, Q. Wang, X. Bai, D. Zu, J. Song, D. Wang, Z. Liu, Z. Li, N. Tao, K. Huang, M. Lei, B. Li, H. Wu, *Npj Flexible Electronics*, 2019, **3**, 6, doi: 10.1038/s41528-019-0050-8.
[32] S. Lin, H. Wang, X. Zhang, D. Wang, D. Zu, J. Song, Z. Liu, Y. Huang, K. Huang, N. Tao, Z. Li, X. Bai, B. Li, M. Lei, Z. Yu, H. Wu, *Nano Energy*, 2019, **62**, 111-116, doi: 10.1016/j.nanoen.2019.04.071.
[33] B. Nie, R. Huang, T. Yao, Y. Zhang, Y. Miao, C. Liu, J. Liu,

X. Chen, *Advanced Functional Materials*, 2019, **29**, 1808786, doi: 10.1002/adfm.201808786.
[34] D. Chen, Y. Cai, M. Huang, *IEEE Sensors Journal*, 2018, **18**, 6337-6344, doi: 10.1109/jsen.2018.2832129.
[35] J. Liu, S. Lin, K. Huang, C. Jia, Q. Wang, Z. Li, J. Song, Z. Liu, H. Wang, M. Lei, H. Wu, *Npj Flexible Electronics*, 2020, **4**, 10, doi: 10.1038/s41528-020-0074-0.
[36] S. Azadi, S. Peng, S. A. Moshizi, M. Asadnia, J. Xu, I. Park, C. H. Wang, S. Wu, *Advanced Materials Technologies*, 2020, **5**, 2000426, doi: 10.1002/admt.202000426.
[37] S. Lin, J. Liu, Q. Wang, D. Zu, H. Wang, F. Wu, X. Bai, J. Song, Z. Liu, Z. Li, K. Huang, B. Li, M. Lei, H. Wu, *Advanced Materials Technologies*, 2020, **5**, 1900761, doi: 10.1002/admt.201900761.
[38] S. Lin, X. Bai, H. Wang, H. Wang, J. Song, K. Huang, C. Wang, N. Wang, B. Li, M. Lei, H. Wu, *Advanced Materials*, 2017, **29**, 1703238, doi: 10.1002/adma.201703238.
[39] S. Hong, Y. Lee, H. Park, S. Jin, Y. Jeong, J. Yun, I. You, G. Zi, J. Ha, *Advanced Materials*, 2016, **28**, 930-935, doi: 10.1002/adma.201504659.

Author Information

Yufeng Wu *received his B.D. at Northeast Normal University in 2015. Now, he is pursuing his Ph.D. in Beijing University of Posts and Telecommunications. His research interest is the fabrication, assembly and application of flexible sensors.*

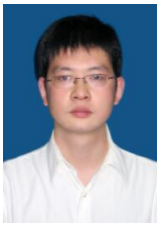

Ming Lei *received his M.D. at State Key Laboratory of Materials Composites and Advanced Technology, Wuhan University of Technology in 2004. Then, he received his Ph.D. from the Laboratory of Nanophysics and Devices, Institute of Physics, Chinese Academy of Sciences in 2007. He worked as a postdoctoral fellow at The Hong Kong University of Science and Technology (2007-2008) and the Chinese University of Hong Kong (2009-2010). He is now a professor and doctoral supervisor of the School of Science, Beijing University of Posts and Telecommunications. He has long been engaged in the preparation of low dimensional nano materials, photoelectric properties and device applications.*

